Evaporation Mechanism of Sn and SnS from Liquid Fe: Part II: Residual Site and Evaporation Kinetics *via* Sn(g) and SnS(g)

SUNG-HOON JUNG, YOUN-BAE KANG, JEONG-DO SEO, JOONG-KIL PARK, and JOO CHOI

Evaporation of Sn from molten steel was experimentally investigated for Fe-Sn-S alloy with low initial S ($0.0007 < [\text{pct S}]_0 < 0.05$) or with high initial S ($0.55 < [\text{pct S}]_0 < 0.894$) at 1873 K (1600 °C) using an electromagnetic levitation melting technique, in order to clarify the role of S on the evaporation mechanism of Sn. It was found that increasing initial S concentration, $[\text{pct S}]_0$, decreased the second-order evaporation rate constant of Sn (k_{SnS}), but there was a residual rate for the evaporation even at high $[\text{pct S}]_0$. The obtained residual rate constant, $k^{\text{r}}_{\text{SnS}}$, was 1.4×10^{-9} m^4 mol^{-1} s^{-1} at 1873 K (1600 °C). Evaporation of Sn under virtually no S condition ($[\text{pct S}]_0 = 0.0007$) was also measured and corresponding first-order rate constant was determined to be 3.49×10^{-7} m s^{-1} at 1873 K (1600 °C). A comprehensive model for the Sn evaporation from molten Fe-Sn-S alloy was developed in the present study, under the condition where mass transfer in gas and liquid phases were fast and interfacial chemical reaction controlled the evaporation of Sn. The model equation is able to represent the evaporation of Sn in the forms of Sn(g) and SnS(g) simultaneously, from very low S melt (when there is no S) to very high S melt investigated in the present study up to ~0.9 mass pct. Gradual transition of major evaporation species from SnS(g) to Sn(g) was well accounted for by the developed model.

DOI: 10.1007/s11663-014-0177-x

I. INTRODUCTION

As shown in a separate article of the present series of articles (Part I), the evaporation of Sn from molten Fe-Sn-S droplet is affected by the presence of S in the melt.[1] It was evident that the evaporation of Sn was accelerated by S, as Sn was evaporated in the form of SnS(g). It was in consistent result with earlier investigations.[2–6] On the other hand, under the condition where mass transfers in the liquid and the gas phases were both fast so they do not limit the evaporation of SnS(g), the evaporation rate was not clearly represented by a second-order reaction of which the rate was simply proportional to [pct Sn] × [pct S]. It was elucidated in the present authors' previous study[1] that S could be adsorbed onto the surface of the droplet, and could block available reaction sites for the evaporation. The adsorption of S was interpreted by applying the Langmuir ideal adsorption isotherm,[7] and it was taken into account in the modification of the rate constant of the evaporation rate equation. The procedure was very similar to that for the decarburization of molten steel containing S by Sain and Belton.[8]

SUNG-HOON JUNG, Graduate Student, and YOUN-BAE KANG, Associate Professor, are with the Graduate Institute of Ferrous Technology, Pohang University of Science and Technology, Pohang, Kyungbuk 790-784, Republic of Korea. Contact e-mail: ybkang@postech.ac.kr JEONG-DO SEO, Senior Principal Researcher, JOONG-KIL PARK and JOO CHOI, Group Leaders, are with the Steelmaking Research Group, Technical Research Laboratories, POSCO, Pohang, Kyungbuk 790-785, Republic of Korea.

Manuscript submitted February 24, 2014.
Article published online September 12, 2014.

In the present article as a second part of the present series, the above investigation is further discussed for the cases: at very low initial S concentration (down to 0.0007 mass pct) or at very high initial S concentration in the Fe-Sn-S liquid alloy up to almost 0.9 mass pct. It is clear that in the absence of S or very limited S available, Sn evaporation in the form of SnS(g) would be unlikely or very limited, but in the form of Sn(g) should be taken into account. On the other hand, at relatively high S concentration where SnS(g) prevails over Sn(g), the previously developed model equation for the evaporation of SnS(g) seemed to underestimate the evaporation rate of SnS(g).[1] According to Sain and Belton[9] who investigated decarburization of molten Fe-C alloy by oxidizing gas blown onto the surface of the molten alloy, there were some sites which could not be blocked by S, and these sites were always available for the decarburization. This was called as *residual sites*. It is of interest whether such residual site concept holds in the present study for SnS(g) evaporation. The present article discusses the above issues employing the same experimental equipment used in Part I.[1] Finally, a comprehensive model for the Sn evaporation from molten Fe-Sn-S alloy is presented, under the condition where mass transfers in gas and liquid phases were fast and interfacial chemical reaction controlled the evaporation of Sn. This model takes into account simultaneous evaporation of Sn(g) and SnS(g). In order to clearly distinguish terms used throughout this article, "evaporation of Sn(g)" is used to mean the evaporation of Sn in the form of Sn(g) exclusively. Similarly, "evaporation of SnS(g)" is used only for the evaporation of Sn in the form of SnS(g). "Overall evaporation

rate'' is used to refer evaporation rate of Sn in both forms, Sn(g) and SnS(g). Third part of the present series will report about the effect of C on the evaporation of Sn.[10]

II. EXPERIMENTAL

Experimental equipment and procedure are the same as those given in the previous article.[1] Fe-Sn-S alloys of various initial compositions were preliminarily prepared in an induction melting furnace under purified Ar atmosphere. Initial sample compositions are listed in Table I. A piece of each of those alloys approximately 6×10^{-4} kg was melted under Ar-4 pct H_2 gas flow (1 L min^{-1}) in an electromagnetic levitation equipment. The temperature of the droplet was monitored by a two-color pyrometer. All experiments were carried out at 1873 K (1600 °C). After a predetermined time, the droplet was quenched into a water-cooled copper mold. The sample was collected, and Sn and S concentrations of the samples were analyzed by Inductively Coupled Plasma spectrometer (ICP-AES, Thermo Scientific ICAP 6500) and C/S combustion analysis method (LECO CS844), respectively.

In particular, samples of the Fe-Sn-S alloys were made in such a way that the alloys contain very low initial S below 0.05 mass pct or even no S (0.0007 mass pct), or relatively high initial S up to 0.894 mass pct. Details of the procedure and schematic diagram of the experimental equipment are shown in Part I.[1]

III. RESULTS

Figures 1 and 2 show decrease of [pct Sn] in molten Fe-Sn-S droplets at 1873 K (1600 °C) at different [pct $S]_0$. Data of the samples having initially less than 0.0615 mass pct of [pct $S]_0$ are shown in Figure 1, while those with higher than 0.1 mass pct of [pct $S]_0$ are shown in Figure 2. As will be shown later, the samples with high initial S ([pct $S]_0 > 0.0615$) exhibit the evaporation of Sn mainly in the form of SnS(g), while those with low initial S ([pct $S]_0 < 0.0615$) show simultaneous evaporation *via* Sn(g) and SnS(g).

Experimental data reported in the previous article ($0.06 \le$ [pct $S]_0 \le 0.39$) are also shown together for comparison.[1] It is clearly seen that the increase of [pct $S]_0$ increased the overall evaporation rate of Sn.

IV. DISCUSSION

In the present authors' previous report,[1] it was shown that Sn evaporated in the form of SnS(g) from liquid Fe-Sn-S liquid alloy where [pct $S]_0$ was in the range of 0.0615 to 0.391. The number of moles of Sn removed from the liquid alloy (Δn_{Sn}) was almost the same as the number of moles of S removed from the liquid alloy (Δn_S) for the case of [pct $S]_0$ = 0.0615. It is expected that Sn in some alloys having [pct $S]_0$ higher than 0.0615 mass pct also should evaporate in the form of SnS(g).

In the present investigation, it is attempted to extend the concentration range of S in order to further clearly elucidate evaporation mechanism of Sn in Fe-Sn-S liquid alloy for wide range of [pct S]. As mentioned in the Section I, absence of S in the liquid alloy will certainly change the species for the evaporation of Sn. Also, it is also to be checked carefully whether there exist residual sites regarding adsorption of S. This will play a role in the development of evaporation rate equation of SnS(g).

A. *Evaporation of Sn in the Form of Sn(g): Very Low or No Initial S*

When there is very low S or virtually no S, Sn would be evaporated in the form of Sn(g):

$$\underline{\mathrm{Sn}} = \mathrm{Sn(g)} \qquad [1]$$

The evaporation rate can be expressed as

$$\frac{d[\text{pct Sn}]}{dt} = -k_{Sn}\frac{A}{V}[\text{pct Sn}] \qquad [2]$$

and integrating the above equation yields

$$\log\frac{[\text{pct Sn}]}{[\text{pct Sn}]_0} = -k_{Sn}\frac{A}{V}t, \qquad [3]$$

where k_{Sn}, A, V, and t are an apparent rate constant of the first-order rate equation (m s^{-1}), reaction area (m^2), volume of the liquid alloy (m^3), and the reaction time (s), and [pct Sn] and [pct $Sn]_0$ are instantaneous and initial concentrations of Sn in the liquid alloy, respectively. It

Table I. Experimental Conditions Employed in the Present Study

Exp. No.	Flow Rate (L min^{-1})	[Pct $Sn]_0$	[Pct $S]_0$	Mass (kg)	Density (kg m^{-3})	Dimension of Droplet	
12	1.0	0.220	0.0007*	$(6 \pm 0.1) \times 10^{-4}$	7000	radius (m)	2.74×10^{-3}
13		0.198	0.010			surface (m_2)	9.40×10^{-5}
14		0.197	0.026			volume (m_3)	8.57×10^{-8}
15		0.188	0.050				
16		0.170	0.554				
17		0.173	0.894				

All experiments were carried out at 1873 K (1600 °C).
*No S was introduced in the sample during the preparation of this sample.

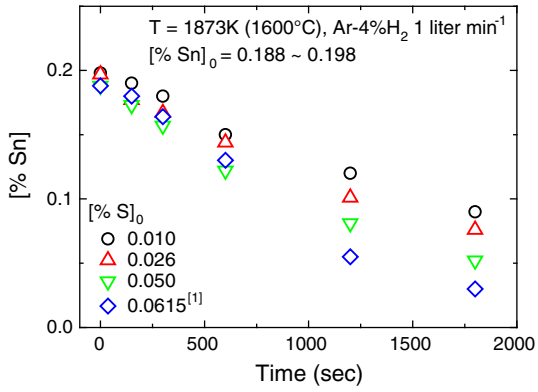

Fig. 1—Decrease of [pct Sn] under [pct S]$_0$ from 0.010 to 0.0615 at 1873 K (1600 °C). [pct Sn]$_0$ = 0.188 to 0.198, flow rate = 1 L min^{-1}, respectively.

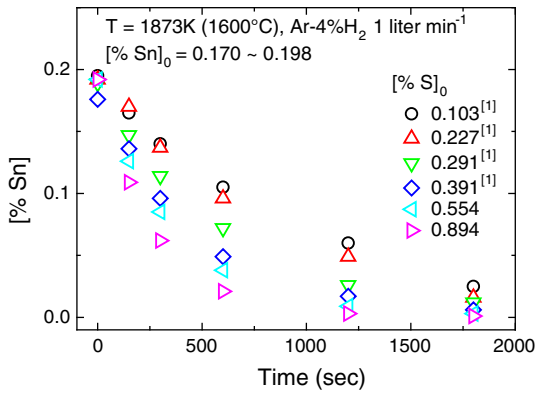

Fig. 2—Decrease of [pct Sn] under [pct S]$_0$ from 0.103 to 0.894 at 1873 K (1600 °C). [pct Sn]$_0$ = 0.170 to 0.198, flow rate = 1 L min^{-1}, respectively.

was assumed that the evaporation of Sn(g) was controlled by the vaporization reaction of Sn, and the apparent rate constant was thought to be the chemical (vaporization) reaction rate constant. However, rate controlling by either gas phase mass transfer or by liquid phase mass transfer would yield the same form of the rate equation.

As described in the previous article,[1] S blocks the reaction sites for the SnS(g) evaporation by the adsorption of S onto the surface of the liquid alloy. In the present study, it is assumed that the same phenomena hold for the present case where Sn evaporates in the form of Sn(g), so as to decrease the rate constant k_{Sn} by the S adsorption. Therefore, the rate constant k_{Sn} in Eqs. [2] and [3] was modified into the following form with the help of Langmuir ideal adsorption isotherm[7]:

$$k_{Sn} = \frac{k_{Sn}^{R}}{1 + K_S[\text{pct S}]}, \qquad [4]$$

where k_{Sn}^{R} and K_S are the chemical reaction rate constant of Sn(g) evaporation of fully open surface (m s^{-1}), and the adsorption coefficient for S, respectively. By plotting the experimental data of virtually no S (0.0007 mass pct) using Eq. [3] as shown in Figure 3, k_{Sn}^{R} was obtained to

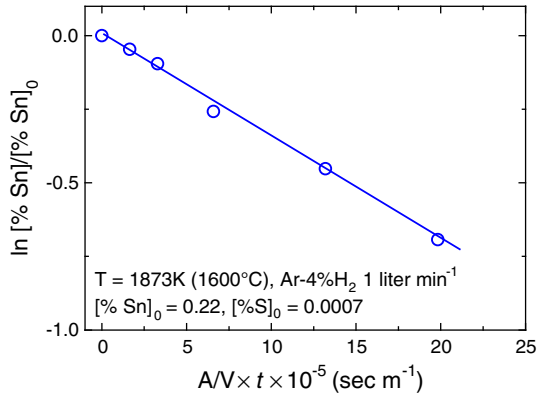

Fig. 3—Representation of the first-order rate equation of Eq. [3] for the liquid alloy where [pct S]$_0$ is virtually zero (0.0007 mass pct).

be 3.49 × 10^{-7} m s^{-1} at 1873 K (1600 °C). This value represents the rate constant of Sn evaporation in the form of Sn(g), in the absence of S in the molten Fe-Sn alloy. Decrease of the k_{Sn} by the adsorption of S is taken into account by Eq. [4] where K_S can be taken from a known literature: 40 at 1873 K (1600 °C).[11]

B. *Residual Rate of Sn Evaporation in the Form of SnS(g): High Initial S*

When Sn evaporates in the form of SnS(g) through the following reaction as described in the previous article[1]:

$$\underline{\text{Sn}}^{i} + \underline{\text{S}}^{i} = \text{SnS}^{i}(g) \qquad [5]$$

corresponding to the chemical reaction at the surface of the liquid alloy, the evaporation rate of SnS(g) can be represented by the following second-order rate equation:

$$\frac{\text{d}[\text{pct Sn}]}{\text{d}t} = -k_{SnS}\frac{A}{V}[\text{pct Sn}][\text{pct S}], \qquad [6]$$

where k_{SnS} is an apparent rate constant of the second-order rate equation (m s^{-1}).

By taking into account a conversion for the concentration unit between mole and mass, and assuming that ideal Langmuir isotherm holds for the adsorption of S[7,8,12]:

$$K_S \cong \frac{\theta_S}{(1-\theta_S)[\text{pct S}]}, \qquad [7]$$

where K_S and θ_S are the adsorption coefficient for S and the fraction of the surface sites occupied by S, the following form of the second-order rate constant was derived[1]:

$$k_{SnS} = \frac{k_{SnS}^{R}}{100M_S}\frac{\rho}{1 + K_S[\text{pct S}]}, \qquad [8]$$

where M_S is molecular weight of S and ρ is the density of the liquid alloy. It was taken into account that reaction area A in Eq. [6] was changed to $A(1 - \theta_S)$ due to the adsorption of S, as described in Part I. In Eq. [8], k_{SnS}^{R}

should be a constant at a given temperature. By analyzing the evaporation kinetics of SnS(g) along with $K_S = 40$,[11] it was reported that k^R_{SnS} was 2.57×10^{-8} m^4 mol^{-1} s^{-1}.[1] Therefore, k_{SnS} can be expressed as a function of [pct S] by Eq. [8].

Open circles in Figure 4 show the rate constant k^R_{SnS} obtained from experimental data in the previous article.[1] They are almost constant regardless of [pct S]$_0$ in the range of 0.06 to 0.29. However, when [pct S]$_0$ increased up to 0.391, the calculated k^R_{SnS} by Eq. [8] (represented by the dashed line) was considerably lower than the experimentally obtained value. In the present study, further experiments were carried out at higher [pct S]$_0$ condition (0.554, 0.894), and using Eqs. [6] and [8], the k^R_{SnS} for the high [pct S]$_0$ samples was obtained and is shown in Figure 4 as closed circles. As can be seen, the evaluated k^R_{SnS}using the experimental data deviates from the dashed line for the constant k^R_{SnS} (2.57×10^{-8} m^4 mol^{-1} s^{-1}[1]) to higher value. This implies that at high [pct S]$_0$, the apparent rate constant k_{SnS} is not as low as what Eq. [8] gives along with the k^R_{SnS} evaluated in the previous report.[1] k_{SnS} given in Eq.

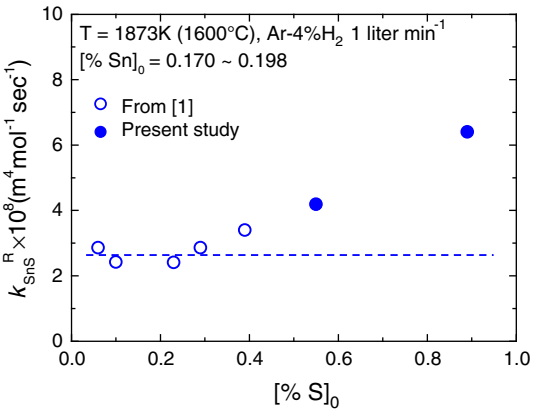

Fig. 4—The chemical reaction rate constant k^R_{SnS} of Eq. [8] extracted from Fig. 2 at different [pct S]$_0$. Dashed line is only to guide the eye to represent the k^R_{SnS} without the consideration of the residual sites. Open circles were taken from,[1] while solid circles were obtained in the present study.

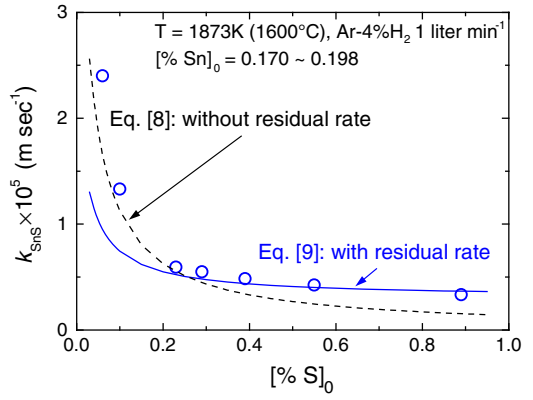

Fig. 5—The apparent second-order rate constant k_{SnS} for liquid alloys of various [pct S]$_0$. Symbols were extracted from the experimental data shown in Fig. 2. Dashed line is calculated using Eq. [8] where the residual sites are not considered. Solid line was calculated by Eq. [9] in the consideration of the residual sites.

[8] is shown in Figure 5 by a dashed curve. The calculated k_{SnS} is very close to the experimental data when [pct S]$_0$ is below 0.3, but starts to underestimate experimentally derived k_{SnS} at higher [pct S]$_0$ (>0.3). Therefore, the rate constant expression of Eq. [8] should be further modified.

As mentioned in Section I of the present article, if there are residual sites on the surface of the Fe-Sn-S liquid alloy which cannot be blocked by S, then the rate constant k_{SnS} can be modified as

$$k_{SnS} = \frac{\rho}{100 M_S}\left(\frac{k^R_{SnS}}{1 + K_S[\text{pct S}]} + k^r_{SnS}\right), \qquad [9]$$

where k^r_{SnS} is the residual rate constant (m^4 mol^{-1} s^{-1}), representing the rate of SnS(g) evaporation even when the surface is saturated by S. Inserting Eq. [9] into Eq. [6] and integrating the equation, assuming $\Delta n_{Sn} = \Delta n_S$ yields

$$\frac{1 + K_S\alpha}{\alpha(1 + \varepsilon + K_S\varepsilon\alpha)} \ln \frac{[\text{pct Sn}]}{[\text{pct Sn}]_0} - \frac{1}{\alpha(1+\varepsilon)} \ln \frac{\beta[\text{pct Sn}] + \alpha}{\beta[\text{pct Sn}]_0 + \alpha} - \frac{K_S}{(1+\varepsilon)(1 + \varepsilon + K_S\varepsilon\alpha)} \ln \frac{1 + \varepsilon + K_S\varepsilon(\beta[\text{pct Sn}] + \alpha)}{1 + \varepsilon + K_S\varepsilon(\beta[\text{pct Sn}]_0 + \alpha)} = -\frac{\rho k^R_{SnS}}{100 M_S}\frac{A}{V}t, \qquad [10]$$

where

$$\alpha = [\text{pct S}]_0 - M_S/M_{Sn}[\text{pct Sn}]_0$$
$$\beta = M_S/M_{Sn}$$
$$\varepsilon = k^r_{SnS}/k^R_{SnS},$$

respectively. Since α and β are all constants for a given [pct S]$_0$, the left hand side (LHS) of Eq. [10] is a function of [pct Sn] provided that ε, the ratio of the residual rate (k^r_{SnS}) over the rate of open surface (k^R_{SnS}) is known. If this is true, plotting the LHS of Eq. [10] as a function of time t should show linear relations. In Figure 6, Eq. [10] was plotted using the experimental data obtained in the present study but only with high [pct S]$_0$ samples (≥0.22). An excellent linear plot was obtained with $\varepsilon = 0.14$.

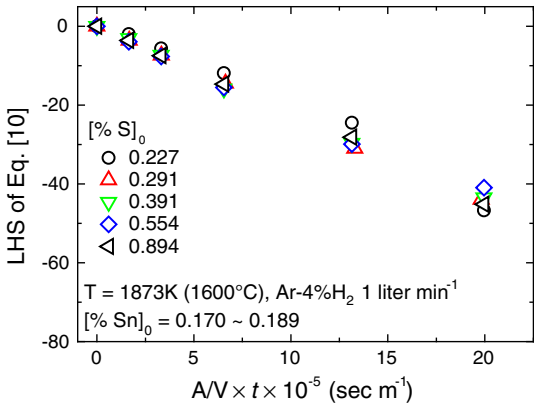

Fig. 6—Representation of the second-order rate equation of Eq. [10]. Adsorption of S and the residual sites are both considered.

Corresponding k^{R}_{SnS} was obtained to be 1.0×10^{-8} m^4 mol^{-1} s^{-1}, which now replaces to the previously reported value (2.57×10^{-8} m^4 mol^{-1} s^{-1}[1]). The residual rate k^{r}_{SnS} was then 1.4×10^{-9} m^4 mol^{-1} s^{-1}. Therefore, the rate equation Eq. [6] with the modified rate constant in Eq. [9] is believed to represent proper evaporation rate of Sn in the form of SnS(g). The ε was found to give a single and linear plot of Eq. [10] regardless of the [pct S]$_0$. Other value for the ε resulted in several linear plots of Eq. [10], with different k^{R}_{SnS} depending on [pct S]$_0$.

The calculated k_{SnS} by Eq. [9] taking into account the residual rate is now shown as a full line in Figure 5. Agreement with the experimentally determined values is excellent when the [pct S]$_0$ is higher than 0.2.

C. *A Comprehensive Model for Overall Evaporation Sn Via Sn(g) and SnS(g)*

Now, the evaporation of Sn from Fe-Sn-S liquid alloy is considered to happen *via* Sn(g) and SnS(g) simultaneously. It is assumed that evaporation in each form is independent each other. Rate equation of the Sn is then expressed as

$$\frac{d[\text{pct Sn}]}{dt} = -\frac{A}{V}(k_{Sn}[\text{pct Sn}] + k_{SnS}[\text{pct Sn}][\text{pct S}]), \quad [11]$$

where k_{Sn} and k_{SnS} were already obtained as Eqs. [4] and [9], respectively. This is a unification of the rate equations of Sn(g) evaporation and SnS(g) evaporation, taking into account the adsorption of S onto the surface and the residual rate.

Contrary to the previous cases where the rate equation of differential form was integrated analytically, Eq. [11] cannot be integrated. This is because it is not possible to assume $\Delta n_{Sn} = \Delta n_S$, as was done in the previous case (Section IV–B) where only SnS(g) evaporation was considered. Therefore, Eq. [11] was solved numerically with a short time step (Δt = 30 seconds). Inserting initial concentrations [pct Sn]$_0$ and [pct S]$_0$ into Eqs. [4], [9] and [11], along with K_S, k^{R}_{Sn}, k^{R}_{SnS}, and k^{r}_{SnS}, the overall rate of decrease of [pct Sn] during a time step Δt is calculated. Also, by comparison between two terms in the parenthesis of Eq. [11], portion of [pct Sn] removed in the form of SnS(g) can be calculated. This allows to calculate how much S was removed in the form of SnS(g). After the time step Δt, new concentrations of [pct Sn] and [pct S] were obtained which can be put again into Eqs. [4], [9] and [11]. All these steps were repeated to calculate [pct Sn] and [pct S] at each time. For example, the [pct Sn] and [pct S] for some samples are shown in Figure 7 as functions of time t along with initial concentrations of Sn and S. Symbols are the

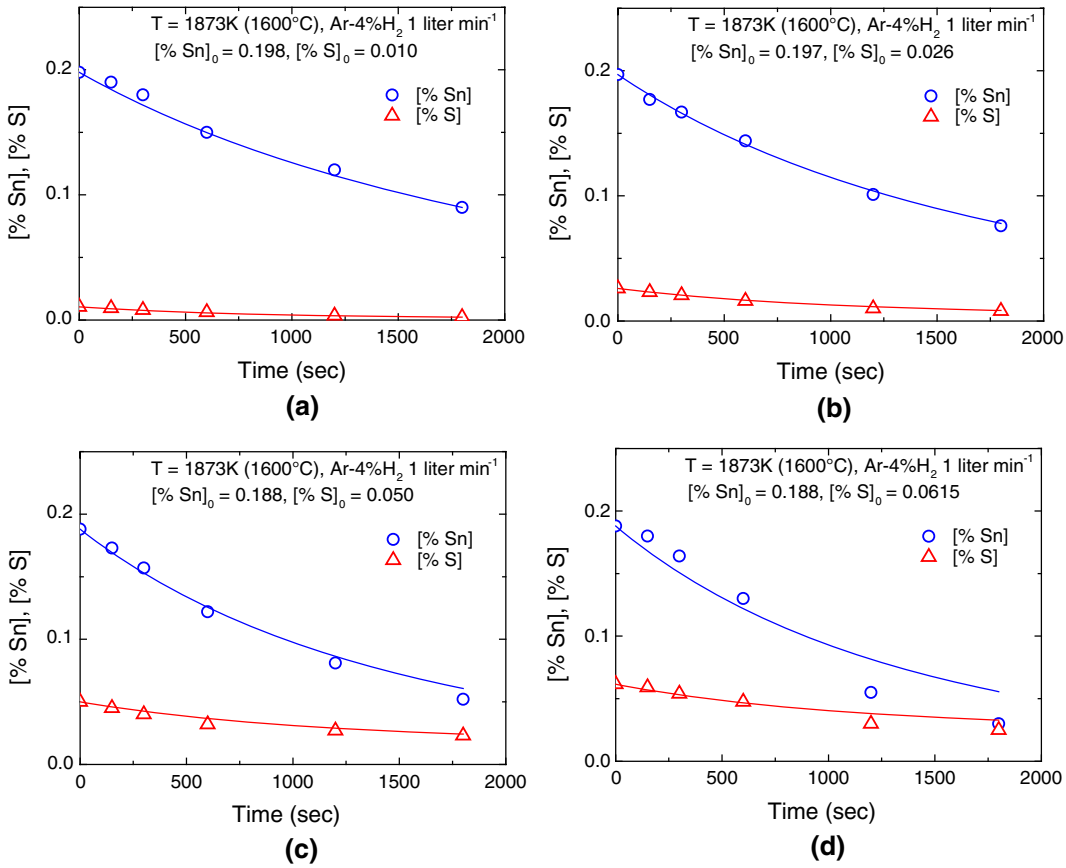

Fig. 7—Decrease of [pct Sn] and [pct S] in several liquid alloys of different initial concentrations: (*a*) [pct Sn]$_0$ = 0.198, [pct S]$_0$ = 0.010, (*b*) [pct Sn]$_0$ = 0.197, [pct S]$_0$ = 0.026, (*c*) [pct Sn]$_0$ = 0.188, [pct S]$_0$ = 0.050, and (*d*) [pct Sn]$_0$ = 0.188, [pct S]$_0$ = 0.0615. Symbols are the experimental data measured in the present study and Part I of the present series.[1] Lines are calculated using the comprehensive model developed in the present study, Eq. [9].

experimental data obtained in the present study as well as those from the previous investigation,[1] while lines are calculated as described above. It is seen that the calculations are indeed in good agreement with the experimental data.

Figure 8 shows the relationship between Δn_{Sn} and Δn_S of the samples used in Figure 7. Symbols are taken from the same source of those in Figure 7, while lines are calculated from the above numerical calculation. It is easily seen that increasing Δn_{Sn} (removed amount of Sn from the liquid alloy) is accompanied with Δn_S (removed amount of S from the liquid alloy). It is interesting to note that the samples with relatively high [pct S]$_0$ (Figures 8(c) and (d)) show $\Delta n_{Sn} \approx \Delta n_S$ at the early stage of evaporation. This represents that Sn is mostly removed in the form of SnS(g). Later stage of the evaporation shows slight deviation from the relation, thus $\Delta n_{Sn} > \Delta n_S$. This tells that gradual depletion of S in the sample changes the mode of evaporation from SnS(g) only to SnS(g) and Sn(g) together. It is more clearly seen for samples with relatively low [pct S]$_0$ (Figures 8(a) and (b)). They show $\Delta n_{Sn} > \Delta n_S$ at the all stage of evaporation. For such samples with insufficient S, the overall evaporation of Sn took place *via* SnS(g) and Sn(g) simultaneously. The model equation developed in the present study does account for this fact.

Figure 9 shows a comparison between experimentally determined [pct Sn] in the samples with various [pct S]$_0$ and calculations in the present study. The calculations well explain the decrease of Sn under various [pct S]$_0$.

Relative portions of Sn(g) and SnS(g) in the overall evaporation of Sn from Fe-Sn-S liquid alloy can also be obtained from the evaporation model developed in the present study. For the demonstration, only initial overall rate of Sn evaporation is considered as the Sn evaporation rate varies as time passes. For a liquid alloy with [pct Sn]$_0$ = 0.2, the initial rate of Sn evaporation (d[pct Sn]$_0$/dt) is shown as a function of [pct S]$_0$ in Figure 10 (full line). The initial rate is seen to increase as [pct S]$_0$ increases. As Eq. [11] shows, the overall rate is contributed by two terms, Sn(g) evaporation and SnS(g) evaporation. Each contribution was calculated by the model and is shown in figure, respectively. The same result for low [pct S]$_0$ is also shown as in Figure 10(b). When there is no S, the overall rate of Sn evaporation is only contributed by the rate of Sn(g) evaporation. However, its contribution to the overall rate of the evaporation becomes low as [pct S]$_0$ increases, while a contribution by SnS(g) evaporation becomes a major

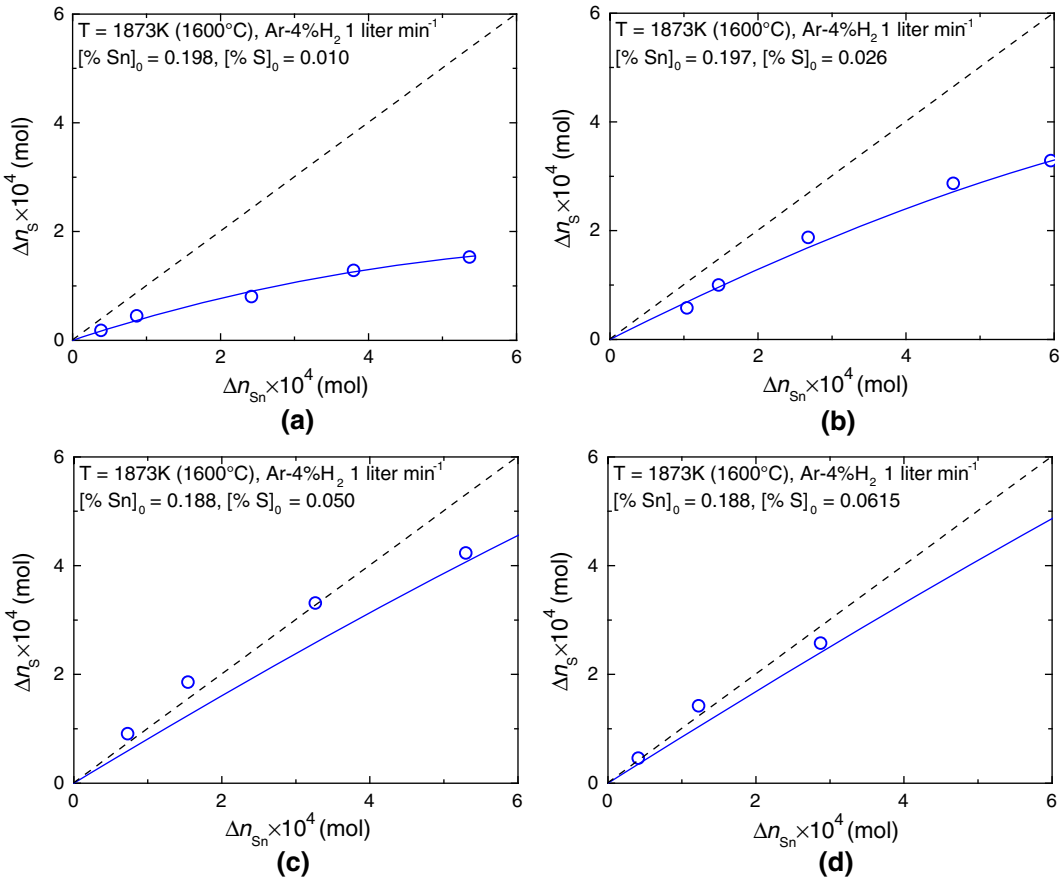

Fig. 8—Number of moles of Sn and S removed from several liquid alloys of different initial concentrations: (*a*) [pct Sn]$_0$ = 0.198, [pct S]$_0$ = 0.010, (*b*) [pct Sn]$_0$ = 0.197, [pct S]$_0$ = 0.026, (*c*) [pct Sn]$_0$ = 0.188, [pct S]$_0$ = 0.050, and (*d*) [pct Sn]$_0$ = 0.188, [pct S]$_0$ = 0.0615. Symbols are the experimental data measured in the present study and Part I of the present series.[1] Lines are calculated using the comprehensive model developed in the present study, Eq. [11].

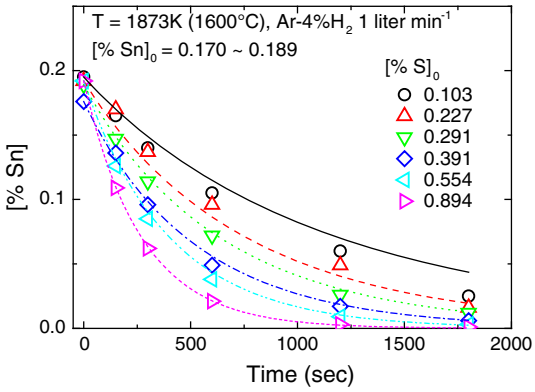

Fig. 9—Comparison between experimentally determined [pct Sn] and the present model calculation, for liquid alloys of different initial concentrations.

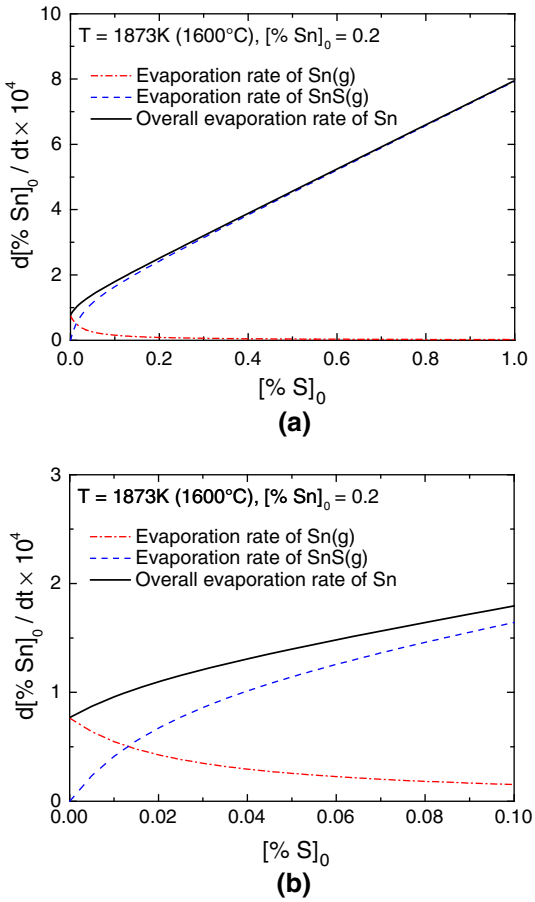

Fig. 10—Calculated evaporation rate of Sn at 1873 K (1600 °C). Evaporation in forms of Sn(g) and SnS(g) is simultaneously considered.

part. Increase of [pct S]$_0$ enhances relative stability of SnS(g) over Sn(g), while it decreases the available sites for the evaporation. This causes the rapid decrease of contribution of Sn(g) evaporation to the overall evaporation rate of Sn.

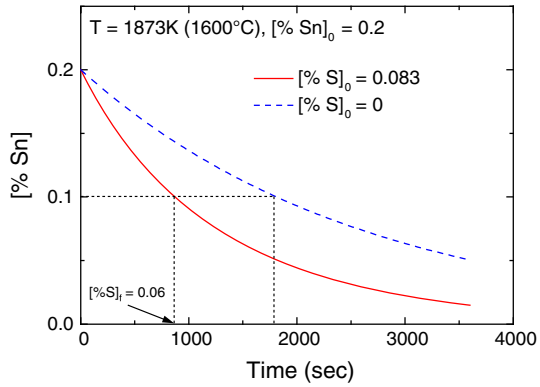

Fig. 11—Predicted change of [pct Sn] in a liquid alloy at 1873 K (1600 °C), in the presence of S (solid line) and in the absence of S (dashed line).

D. *S Content Control for Efficient Removal of Sn*

One of the most important factors for a refining process of Sn removal by the evaporation to be practiced is accelerating the overall evaporation rate of Sn as fast as possible. As discussed throughout the present article, S plays an important role in the acceleration of the evaporation rate. On the other hand, a final S content after the process should be lower than a level that can be readily desulfurized by a conventional desulfurizing process. Therefore, it is necessary to find an optimal S (Figure 11).

As an example, an optimal [pct S]$_0$ was calculated under the condition employed in the present experimental study. It is assumed that [pct Sn]$_0$ is 0.2 mass pct and final S content ([pct S]$_f$) is 0.06 mass pct, after 50 pct of Sn removal at 1873 K (1600 °C). The 0.06 mass pct of [pct S]$_f$ is a typical S level in hot metal after ironmaking process. Calculation using the model of the present study shows that 0.083 mass pct of [pct S]$_0$ is the optimal value for the initial S content in the liquid alloy. After the 50 pct removal of Sn, [pct S]$_0$ of 0.083 mass pct decreases to [pct S]$_f$ of 0.06 mass pct. The time required for 50 pct removal of Sn is 870 seconds, and this is 2.1 times faster than the case where [pct S]$_0$ is zero. The reaction time would be accelerate further by applying vacuum technology.[4,13] Nevertheless, it is thought that the effect of S on Sn removal would not be altered even under the vacuum condition.

V. CONCLUSIONS

Following the present authors' investigation on Sn evaporation from molten steel containing medium level of S,[1] removal of Sn from the molten steel was further investigated for the steel with wide range of [pct S], from 0.0007 mass pct to 0.894 mass pct. The following conclusions were obtained.

1. Evaporation rate of Sn in the absence of S could be represented by the first-order reaction.
2. Evaporation of Sn in the presence of high S should be interpreted with the adsorption of S onto the surface,

along with residual sites by Eq. [9]. k^{R}_{SnS} representing the evaporation chemical reaction rate constant was obtained to be 1.0×10^{-8} m^4 mol^{-1} s^{-1}, while k^{r}_{SnS}, representing the evaporation through residual sites, was 1.4×10^{-9} m^4 mol^{-1} s^{-1} at 1873 K (1600 °C), respectively.

3. A comprehensive model equation for the evaporation of Sn in the forms of Sn(g) and SnS(g) together was developed for the first time. Not only a good accordance with the experimental data was obtained, but also relative portions of Sn(g) and SnS(g) evaporations could be analyzed.
4. The developed model can be applied to design an optimum melt composition for faster Sn removal from molten steel.

ACKNOWLEDGMENTS

This research was financially supported by POSCO Ltd. through Steel Innovation Program.

NOMENCLATURE

ρ	Density of liquid alloy, kg m^{-3}
A	Area of reaction surface, m^2
i	Species i dissolved in liquid alloy
i^{i}	Species i at the interface
[pct i]	Mass percent of species i in liquid alloy at time t
[pct i]$_0$	Mass percent of species i in liquid alloy at initial state ($t = 0$)
k_{Sn}	Apparent rate constant of a first-order reaction, m s^{-1}
k^{R}_{Sn}	Chemical reaction rate constant of the Reaction Sn = Sn(g) when surface of liquid alloy is fully open, m s^{-1}
k_{SnS}	Apparent rate constant of a second-order reaction, m s^{-1}
k^{R}_{SnS}	Chemical reaction rate constant of the Reaction $\underline{Sn}^{i} + \underline{S}^{i} = SnS(g)^{i}$ when surface of liquid alloy is fully open, m^4 mol^{-1} s^{-1}
k^{r}_{SnS}	Residual rate constant of the Reaction $\underline{Sn}^{i} + \underline{S}^{i} = SnS(g)^{i}$, m^4 mol^{-1} s^{-1}
K_S	Adsorption coefficient of S
M_i	Molecular weight of element i, kg mol^{-1}
n_i	Number of moles of species i, mol
t	Reaction time, s
V	Volume of liquid alloy, m^3

REFERENCES

1. S.-H. Jung, Y.-B. Kang, J.-D. Seo, J.-K. Park, and J. Choi: *Metall. Mater. Trans. B*, 2014, DOI:10.1007/s11663-014-0163-3.
2. V.D. Sehgal: *J. Iron Steel Inst*., 1970, vol. 208, pp. 382–86.
3. R.D. Morales and N. Sano: *Ironmak. Steelmak*., 1982, vol. 9, pp. 64–76.
4. L. Savov and D. Janke: *ISIJ Int*., 2000, vol. 40, pp. 654–63.
5. X. Liu and J.H.E. Jeffes: *Ironmak. Steelmak*., 1988, vol. 15, pp. 21–26.
6. X. Liu and J.H.E. Jeffes: *Ironmak. Steelmak*., 1988, vol. 15, pp. 27–32.
7. I. Langmuir: *J. Am. Chem. Soc*., 1918, vol. 40, pp. 1361–1403.
8. D.R. Sain and G.R. Belton: *Metall. Trans. B*, 1976, vol. 7B, pp. 235–44.
9. D.R. Sain and G.R. Belton: *Metall. Trans. B*, 1978, vol. 9B, pp. 403–07.
10. S.-H. Jung, Y.-B. Kang, J.-D. Seo, J.-K. Park, and J. Choi: unpublished research, 2014.
11. K. Sekino, T. Nagasaka, and R.J. Fruehan: *ISIJ Int*., 2000, vol. 40, pp. 315–21.
12. H.-G. Lee and Y.K. Rao: *Metall. Trans. B*, 1982, vol. 13B, pp. 411–21.
13. L. Savov and D. Janke: *ISIJ Int*., 2000, vol. 40, pp. 95–104.